

INVENTORY OF SUPPLEMENTAL INFORMATION

Regulation of epithelial plasticity determines metastatic organotropism in pancreatic cancer

Maximilian Reichert, Basil Bakir, Leticia Moreira, Jason R. Pitarresi, Karin Feldmann, Lauren Simon, Kensuke Suzuki, Ravikanth Maddipati, Andrew D. Rhim, Anna M. Schlitter, Mark Kriegsmann, Wilko Weichert, Matthias Wirth, Kathleen Schuck, Günter Schneider, Dieter Saur, Albert B. Reynolds, Andres Klein-Szanto, Burcin Pehlivanoglu, Bahar Memis, N. Volkan Adsay, and Anil K. Rustgi

SUPPLEMENTAL FIGURES:

Figure S1, related to Figure 1: *p120ctn* is required for both exocrine compartment homeostasis and regeneration after pancreatitis.

Figure S2, related to Figure 1: P120CTN and E-CADHERIN remain co-localized at the membrane in PanIN lesions and PDAC.

Figure S3, related to Figure 2: Circulating tumor cells from KPCY mice differ in their epithelial characteristics based on whether they are single cells or clusters.

Figure S4, related to Figure 4: *Kras^{G12D}; Rosa26^{YFP} (KY)* cells demonstrate the ability to colonize the lung regardless of *p120ctn* status.

Figure S5, related to Figure 5: *Kras^{G12D/wt}; p120ctn^{wt/fl}; Rosa26^{YFP} (KYp120^{wt/fl})* cells give rise to both solid and cystic lesions.

Figure S6, related to Figure 6: P120CTN and E-CADHERIN expression in human IPMN and pancreatic neuroendocrine tumors.

Figure S7, related to Figure 7: Metastatic organotropism is dependent on epithelial-mesenchymal plasticity in multiple genetic and implantation models of pancreatic cancer.

SUPPLEMENTAL TABLES:

Table S1, related to Figure 1: Delineation of 32 *Pdx1-cre*; *Kras*^{G12D/wt}; *Rosa26*^{YFP} mice characteristics

Table S2, related to Figure 1: Delineation of 38 *Pdx1-cre*; *Kras*^{G12D/wt}; *p120ctn*^{wt/fl}; *Rosa26*^{YFP} mice characteristics

Table S3, related to Figure 2: Quantification of metastatic lesions in 18 *Pdx1-cre*; *Kras*^{G12D/wt}; *p53*^{wt/fl}; *Rosa26*^{YFP} mice

Table S4, related to Figure 2: Quantification of metastatic lesions in 10 *Pdx1-cre*; *Kras*^{G12D/wt}; *p53*^{wt/fl}; *p120ctn*^{wt/fl}; *Rosa26*^{YFP} mice

Table S5, related to Figure 5: Delineation of characteristics of long-term orthotopic transplantation with *Kras*^{G12D/wt}; *p120ctn*^{fl/fl}; *Rosa26*^{YFP} cells

Table S6, related to Figure 5: Delineation of characteristics of long-term orthotopic transplantation with *Kras*^{G12D/wt}; *p120ctn*^{fl/fl}; *Rosa26*^{YFP} cells rescued with the p120ctn1A isoform

Table S7, related to Figure 6: Characteristics of Human Tumor Microarray

Supplemental Figure Legends

Figure S1, related to Figure 1: *p120ctn* is required for both exocrine compartment homeostasis and regeneration after pancreatitis. A. Genetic schematic of *Pdx1-cre; p120ctn^{fl/fl}; Rosa26^{YFP}* mice. **B.** P120CTN (green) is lost in a mosaic fashion in the ductal compartment as well as acinar compartment. **C.** Relative amylase levels are significantly decreased in three independent age-matched cohorts (n = 3 per genotype per time interval). T-test. **D.** Representative histology of *Pdx1-cre; p120ctn^{wt/wt}*, *Pdx1-cre; p120ctn^{wt/fl}*, and *Pdx1-cre; p120ctn^{fl/fl}* mice (60-, 74-, and 55-weeks of age, respectively) and P120CTN/E-CADHERIN staining of the acinar and endocrine compartments. Note that whereas P120CTN and E-CADHERIN are localized at the membrane in mice with either wild-type or heterozygous *p120ctn*, homozygous *p120ctn* loss results in fatty degeneration surrounding solitary islets. **E.** Unlike the exocrine compartment of *Pdx1-cre; p120ctn^{fl/fl}* mice, recombined islets (as indicated by YFP+ staining) appear to not require P120CTN for normal architecture. **F.** Pancreata of *Pdx1-cre; p120ctn^{fl/fl}* mice are atrophic 7 days post-pancreatitis induction. **G.** Whereas wild-type have recovered 7 days post-pancreatitis induction, *Pdx1-cre; p120ctn^{fl/fl}* mice show persistent edema, inflammation, and acinar-to-ductal metaplasia (as shown by DBA staining). *Pdx1-cre; p120ctn^{wt/fl}* mice show an intermediate phenotype. **H.** 3 mice per genotype per time point (with the exception of day 1 and 3 of mice with bi-allelic *p120ctn* loss, where only 2 mice were analyzed) were analyzed for edema, inflammation, vacuolization, and necrosis based upon a published pancreatitis scoring system (Rongione et

al., 1997). Three high-powered fields per mouse. Mice with *bi-allelic* p120ctn loss showed significantly impaired regenerative capability 7-days post-induction. Multiple t-tests with Holm-Sidak Correction and assumed equivalent scatter. 50 μ m scale bar for histology. 10 mm for gross pathology.

Figure S2, related to Figure 1: P120CTN and E-CADHERIN remain co-localized at the membrane in PanIN lesions and PDAC. A. Spectrum of pancreatic lesions in *Pdx1-cre; Kras^{G12D/wt}; Rosa26^{YFP}* (KCY) (n = 32) and *Pdx1-cre; Kras^{G12D}; p120ctn^{wt/fl}; Rosa26^{YFP}* (KCYp120^{wt/fl}) (n = 38) mice expressed as a percentage of total mice in each cohort. **B.** P120CTN, E-CADHERIN, and YFP staining of *KCY* and *KCYp120^{wt/fl}* mice show co-localization of P120CTN and E-CADHERIN at all stages of disease. 50 μ m scale bar. (1:50 ECad; 1:250 p120; 1:250 YFP)

Figure S3, related to Figure 2: Circulating tumor cells from KPCY mice differ in their epithelial characteristics based on whether they are single cells or clusters. A. Single cells or clusters of circulating tumor cells were stained for E-CADHERIN, P120CTN, and YFP. **B.** Single cells or clusters of circulating tumor cells were stained for E-CADHERIN, β -CATENIN, and YFP. **C.** Clusters of circulating tumor cells were stained for CYTOKERATIN-19. 10 μ m scale bar.

Figure S4, related to Figure 4: *Kras*^{G12D}; *Rosa26*^{YFP} (KY) cells demonstrate the ability to colonize the lung regardless of *p120ctn* status. A.

Representative FACS plots (x=GFP/YFP; y=FSC) of PDCs with indicated genotypes. YFP positive (YFP+) PDC lines (n=9) were derived from age-matched mice (6-15 weeks). In vitro lentiviral Cre-recombination was performed after a given PDC line was established. Phase-contrast photographs of 9 independently derived KY lines with different *p120ctn* status: *p120ctn*^{wt/wt}, *p120ctn*^{wt/fl}, *p120ctn*^{fl/fl}. **B.** Athymic nude mice were retro-orbitally injected with 750,000 cells from these genotypes and harvested 21 days post-injection. 50 μm scale bar for histology.

Figure S5, related to Figure 5: *Kras*^{G12D/wt}; *p120ctn*^{wt/fl}; *Rosa26*^{YFP} (*KYp120*^{wt/fl}) cells give rise to both solid and cystic lesions. A. Athymic nude mice were orthotopically injected with *KYp120ctn*^{wt/fl} cells and harvested 101 to 180 days post-implantation. Lesions were classified, based on both gross pathology and histology, as to whether they were solid, cystic, or mixed. 4/12 mice had no tumor penetrance. **B.** Athymic nude mice were orthotopically injected with *KYp120ctn*^{wt/fl} cells and harvested 180 days post-implantation. Gross pathology was markedly different, with either solid tumors or clear fluid-filled cystic lesions. 1 mm scale bar for gross pathology. 50 μm scale bar for histology.

Figure S6, related to Figure 6: P120CTN and E-CADHERIN expression in human IPMN and pancreatic neuroendocrine tumors. A. P120CTN expression in human IPMN. Multiple histological subtypes of human IPMN, including gastric-type, intestinal-type, and pancreatobiliary (PB)-type, and unspecified IPMN were stained for P120CTN. Binomial test. **B.** P120CTN expression in human IPMN. **C.** E-CADHERIN intensity is higher in the membranous compartment compared to the cytoplasmic compartment in human IPMN. Wilcoxon Test. **D.** E-CADHERIN expression in human IPMN. **E.** Comparison of localization in human PNET (n = 9) for P120CTN and E-CADHERIN. P120CTN was membranous (M) in 0/9 samples, whereas it was cytoplasmic (C) in 7/9 with or without nuclear (N) staining. E-CADHERIN was demonstrated an absence of any purely membranous samples. Binomial Test. **F.** E-CADHERIN intensity is higher in the cytoplasmic compartment than at the membrane in human PNET. Wilcoxon Test. **G.** Normal human pancreas (n = 2), taken from non-affected tissue adjacent to PNET, shows robust membranous P120CTN and E-CADHERIN localization in both acini and ducts. Interestingly, islets appear to have less membranous staining than the exocrine pancreas. **H.** PNET demonstrates minimal membranous staining for either P120CTN or E-CADHERIN. Scale bar: 50 μ m. *p < .05, **p < .01, ***p < .001.

Figure S7, related to Figure 7: Metastatic organotropism is dependent on epithelial-mesenchymal plasticity in multiple genetic and implantation models of pancreatic cancer.

Supplemental Table Legends

Table S1, related to Figure 1: Delineation of 32 *Pdx1-cre; Kras^{G12D/wt}; Rosa26^{YFP}* mice characteristics

Mouse ID, age, pathological state, and notes for all 32 *Pdx1-cre; Kras^{G12D/wt}; Rosa26^{YFP}* analyzed. PanIN, Pancreatic Intraepithelial Neoplasia. IPMN, Intraductal Papillary Mucinous Neoplasm.

Table S2, related to Figure 1: Delineation of 38 *Pdx1-cre; Kras^{G12D/wt}; p120ctn^{wt/fl}; Rosa26^{YFP}* mice characteristics

Mouse ID, age, pathological state, and notes for all 38 *Pdx1-cre; Kras^{G12D/wt}; p120ctn^{wt/fl}; Rosa26^{YFP}* analyzed. PanIN, Pancreatic Intraepithelial Neoplasia. MCN, Mucinous Cystic Neoplasm. IPMN, Intraductal Papillary Mucinous Neoplasm.

Table S3, related to Figure 2: Quantification of metastatic lesions in 18 *Pdx1-cre; Kras^{G12D/wt}; p53^{wt/fl}; Rosa26^{YFP}* mice

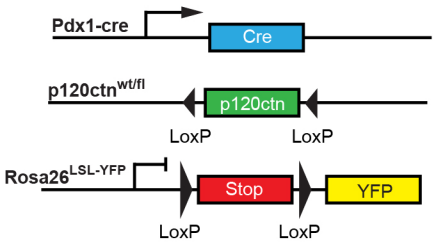
Table S4, related to Figure 2: Quantification of metastatic lesions in 10 *Pdx1-cre; Kras^{G12D/wt}; p53^{wt/fl}; p120ctn^{wt/fl}; Rosa26^{YFP}* mice

Table S5, related to Figure 5: Delineation of characteristics of long-term orthotopic transplantation with *Kras^{G12D/wt}; p120ctn^{fl/fl}; Rosa26^{YFP}* cells

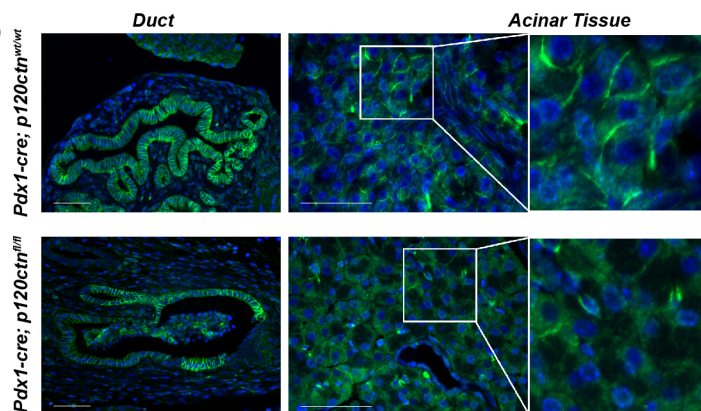
Table S6, related to Figure 5: Delineation of characteristics of long-term orthotopic transplantation with *Kras*^{G12D/wt}; *p120ctn*^{fl/fl}; *Rosa26*^{YFP} cells rescued with the p120ctn1A isoform

Table S7, related to Figure 6: Characteristics of Human Tumor Microarray

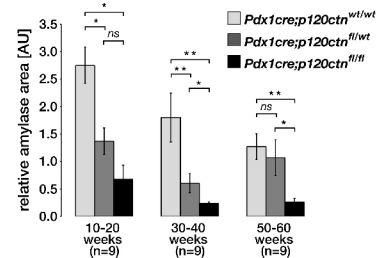
A *Pdx1-cre; p120ctn^{wt/fl}; Rosa26^{LSL-YFP}*



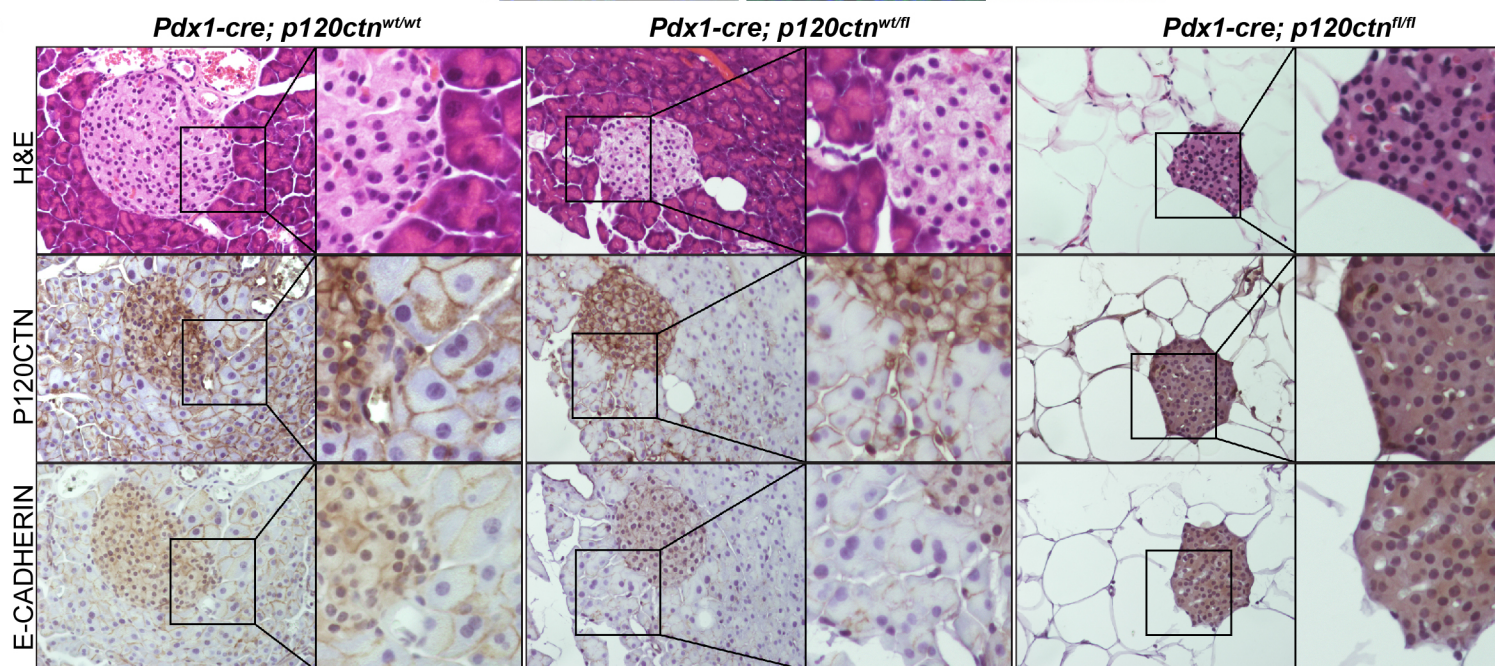
B



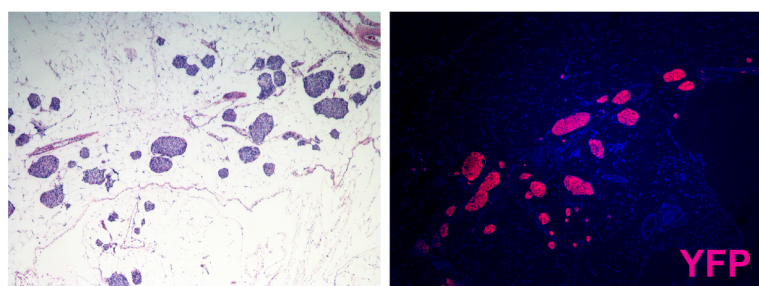
C



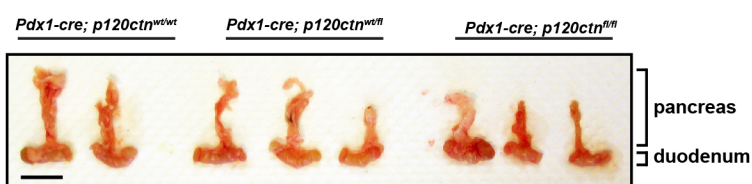
D



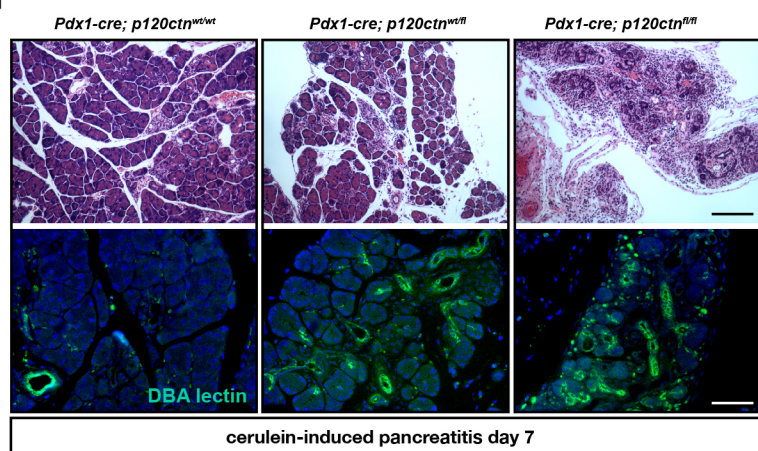
E



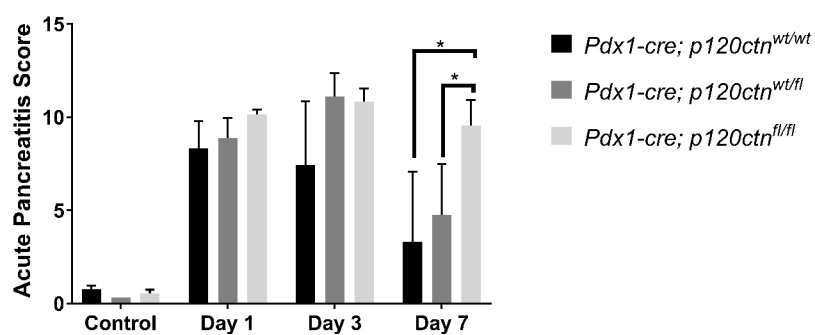
F



G



H



B

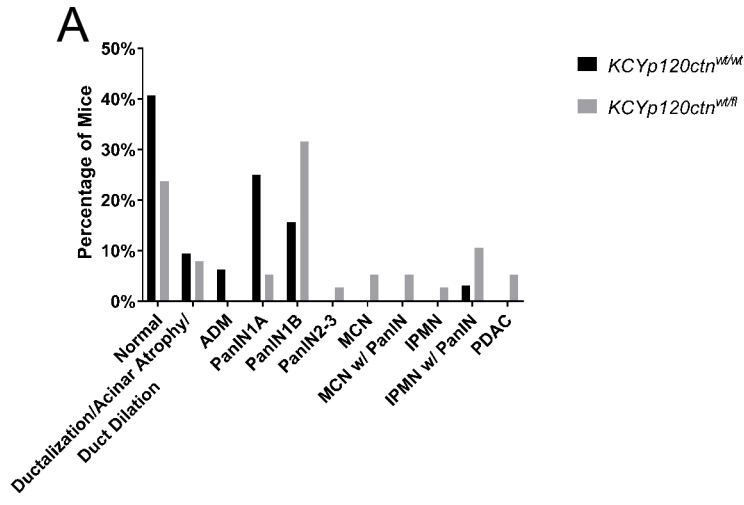
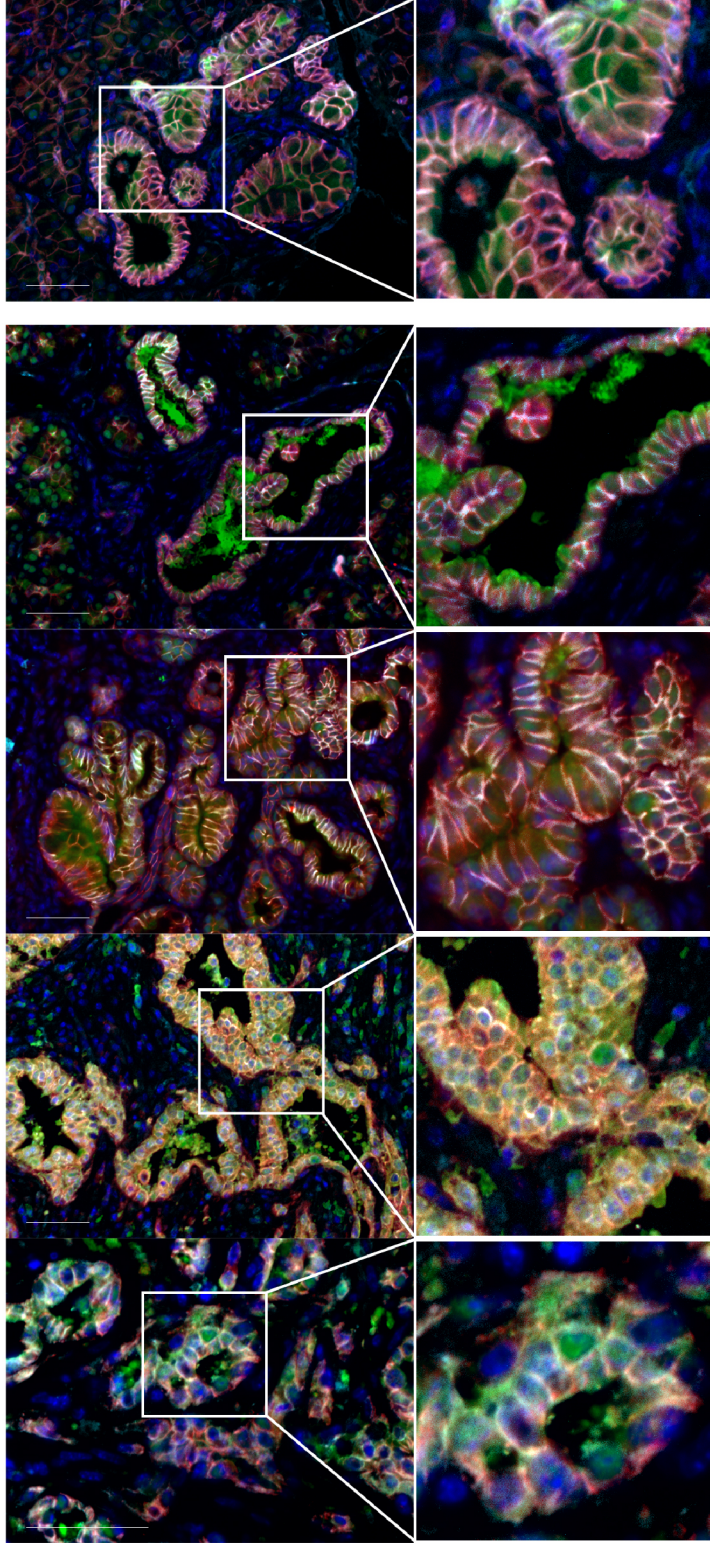
Pdx1-cre; KRAS^{G12D/wt}; Rosa26^{YFP}

Pdx1-cre; KRAS^{G12D/wt}; p120ctn^{wfl/fl}; Rosa26^{YFP}

Adenocarcinoma - 20 weeks of age

Liver Metastasis

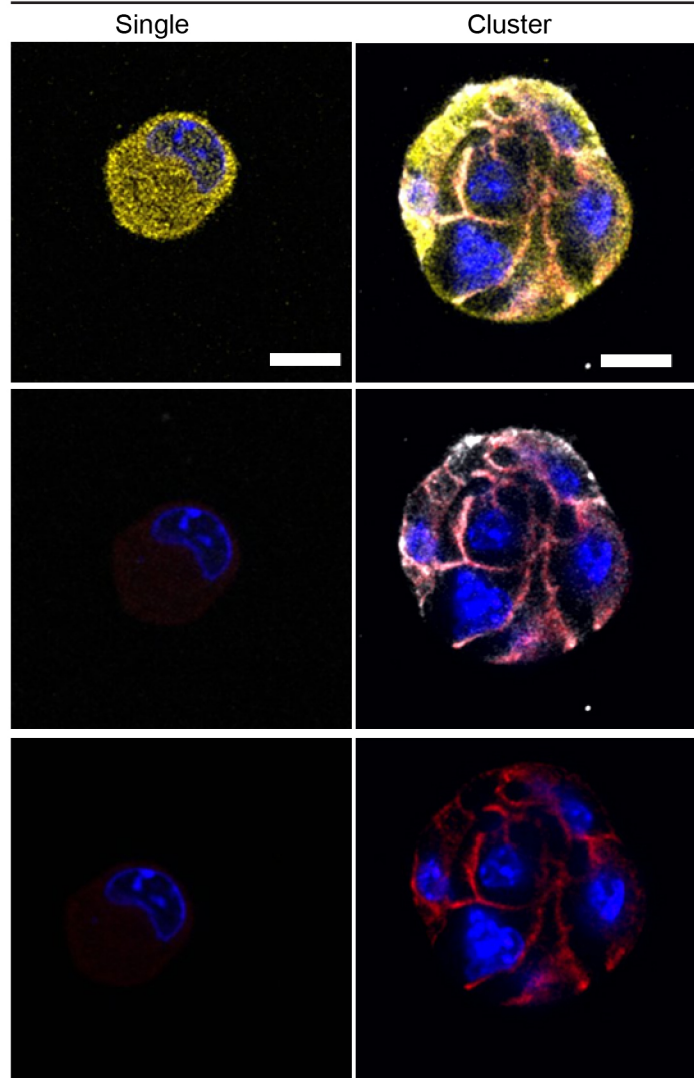
Primary Tumor



Red - E-CADHERIN
 Green - YFP
 Cyan - P120CTN
 Blue - DAPI

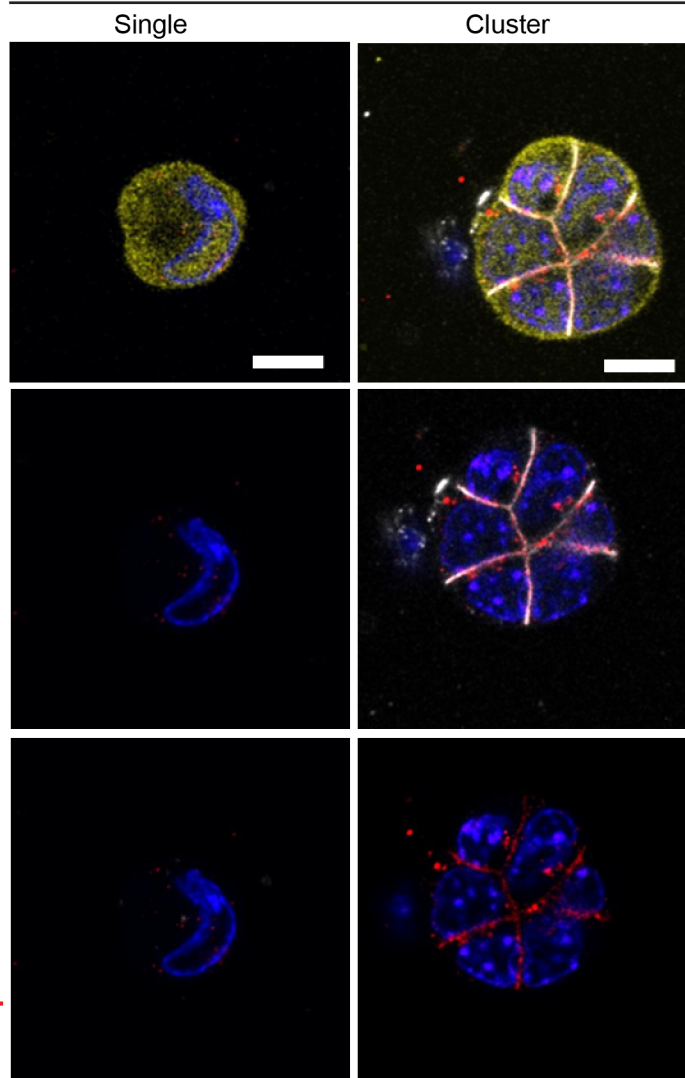
A

P120CTN/YFP/DAPI
E-CADHERIN IN WHITE



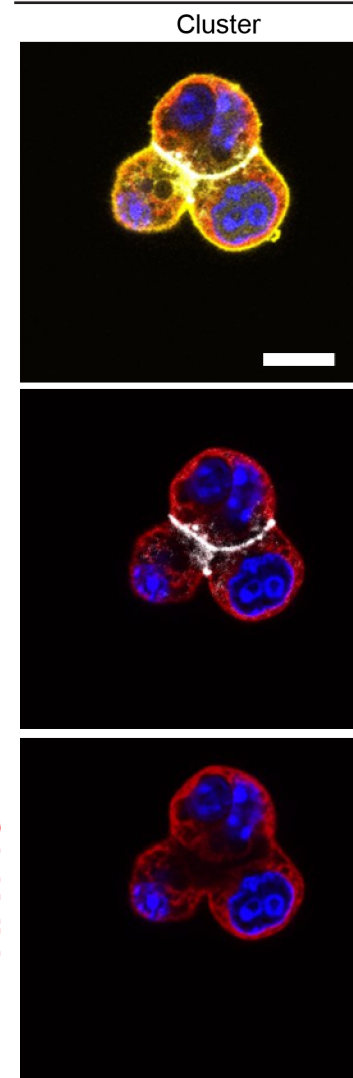
B

β -CATENIN/YFP/DAPI
E-CADHERIN IN WHITE

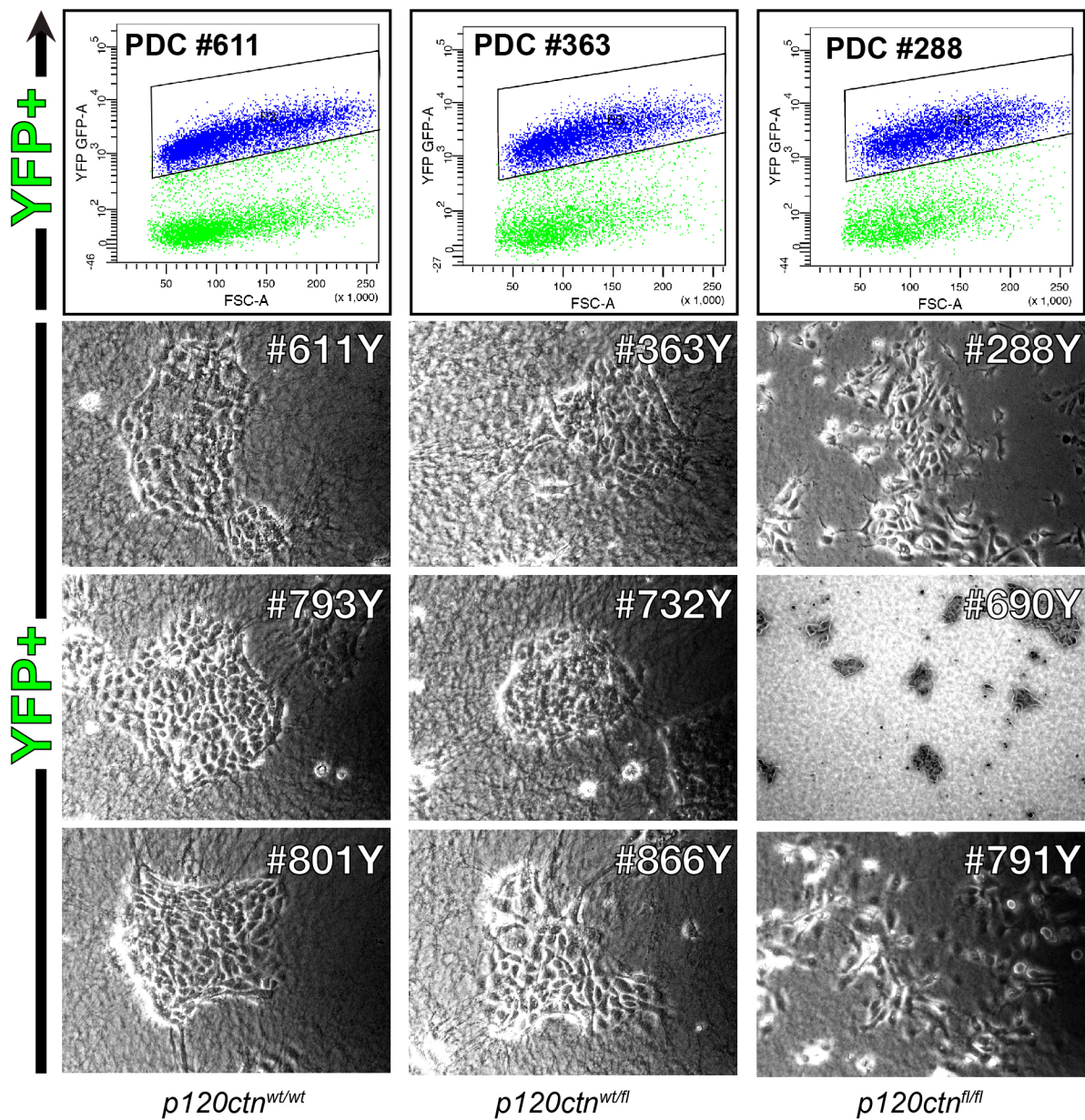


C

B-CATENIN/YFP/DAPI
E-CADHERIN IN WHITE



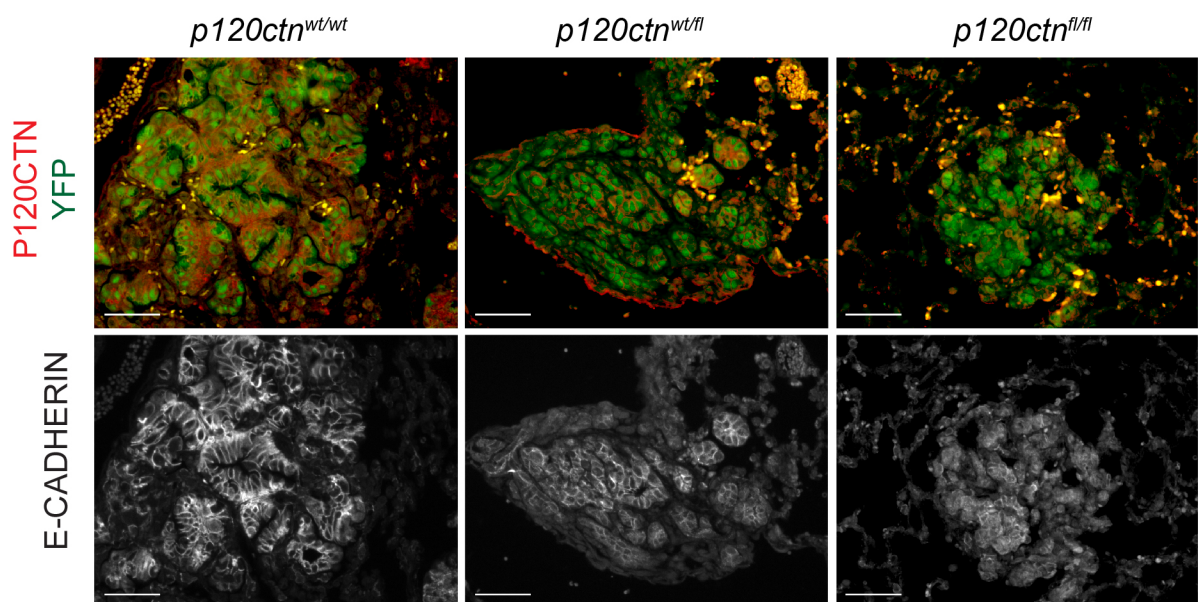
A

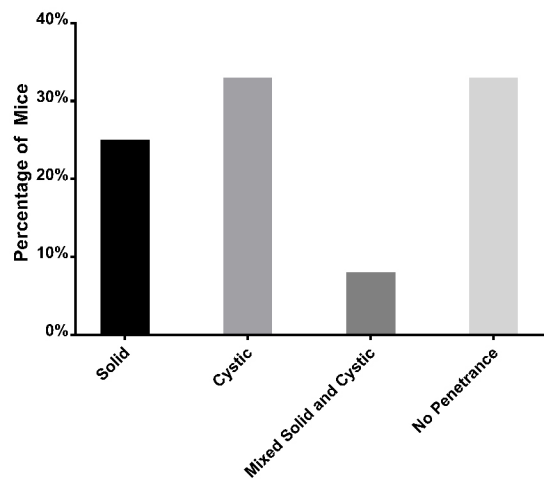


Kras^{G12D/wt}; Rosa26^{YFP}

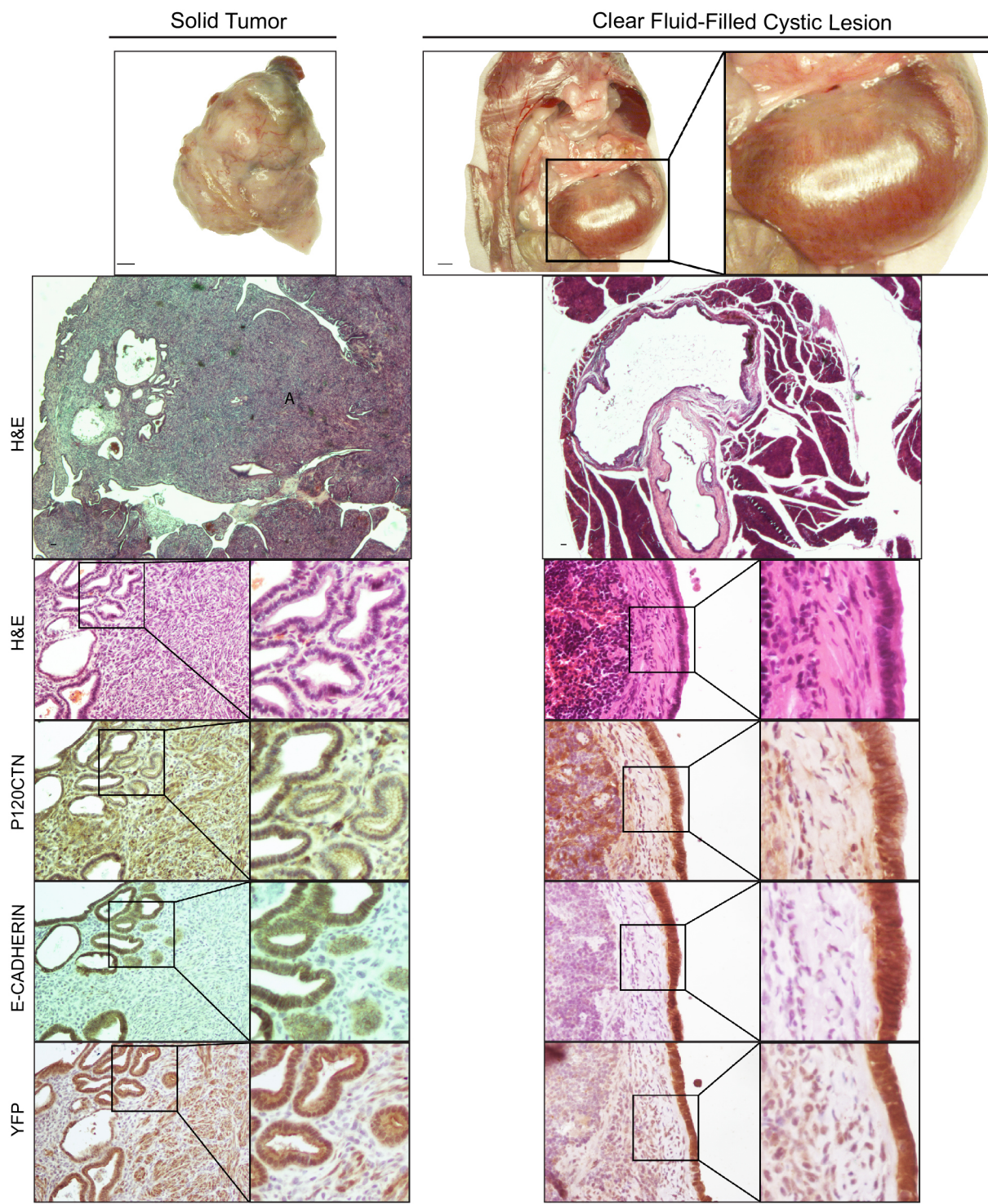
B

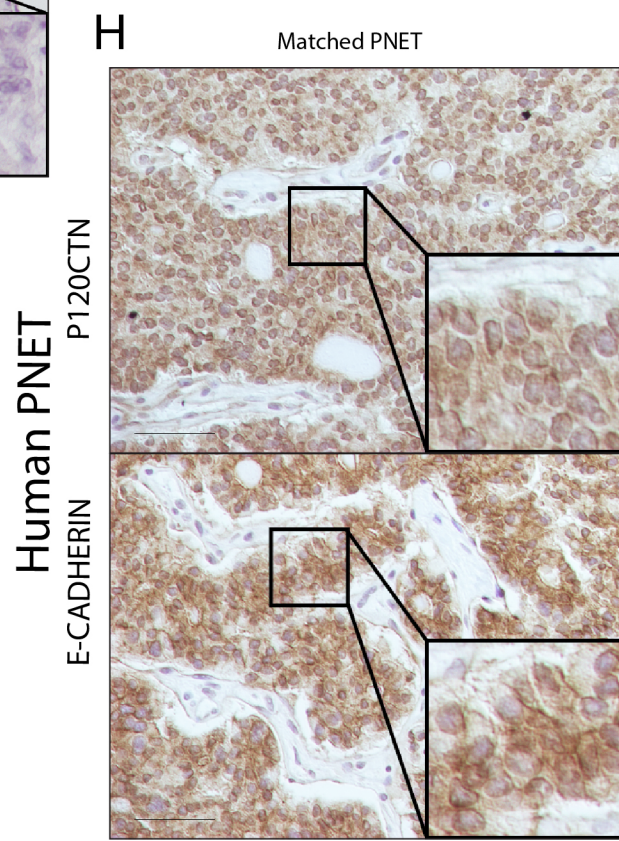
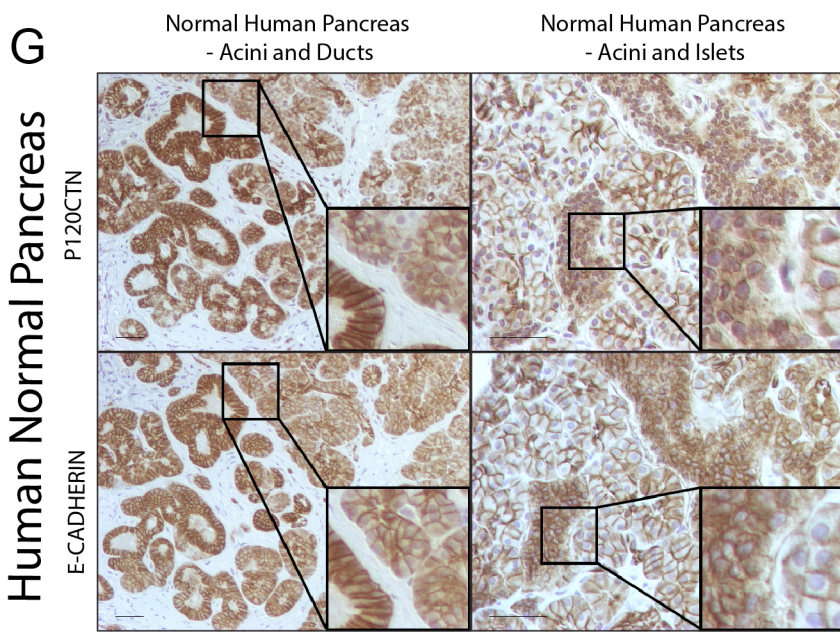
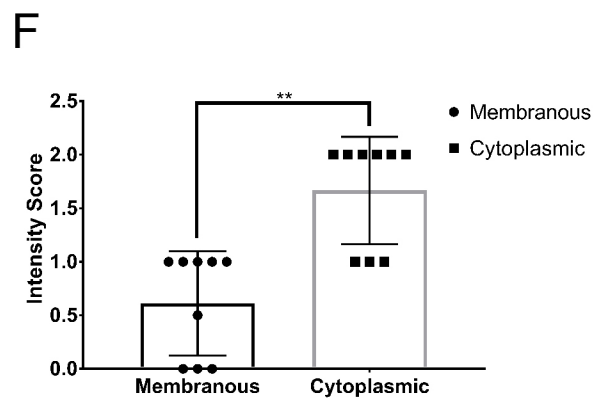
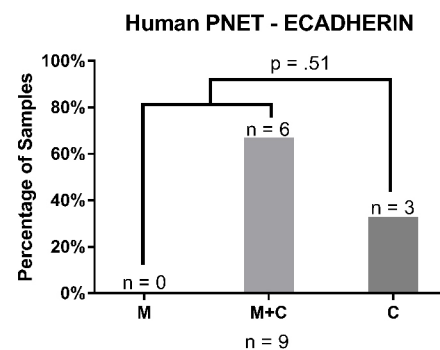
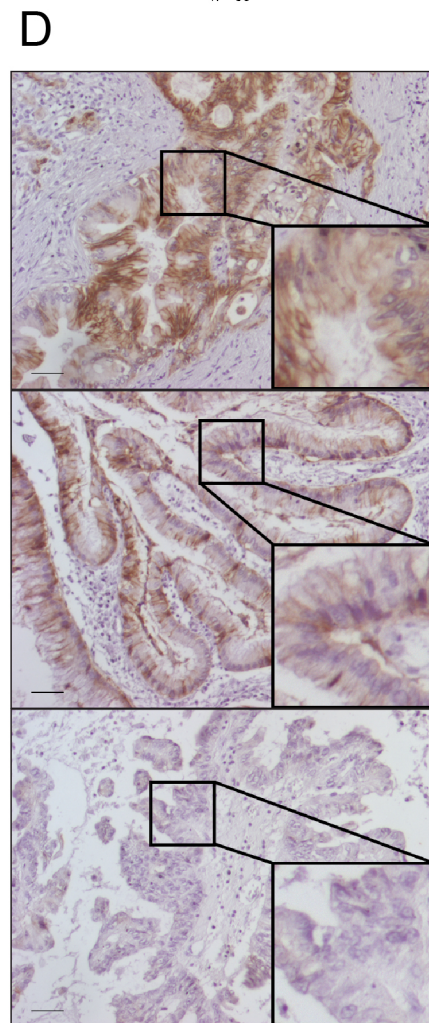
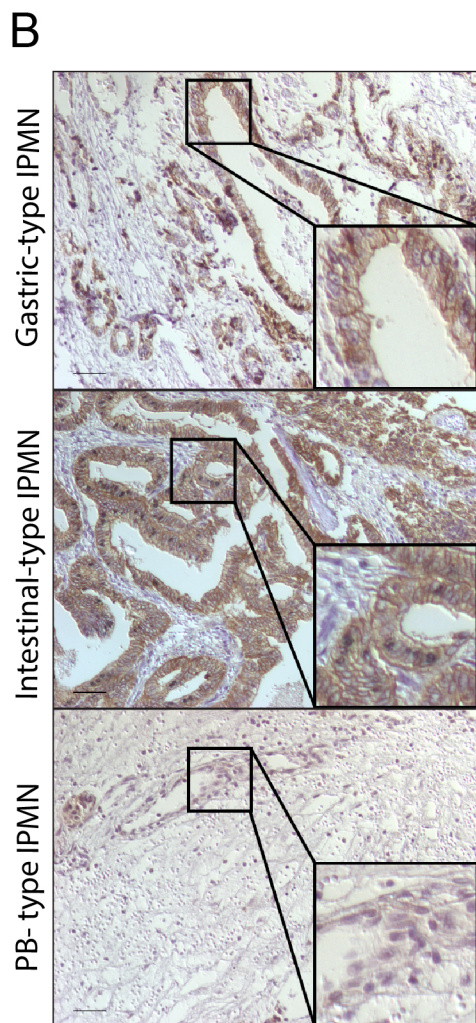
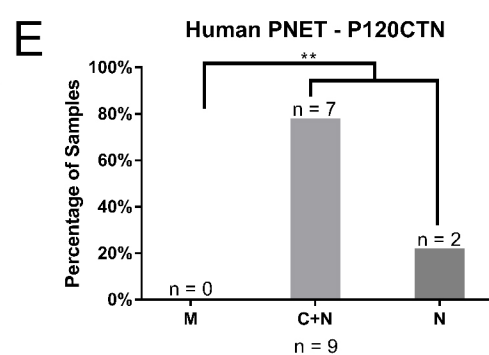
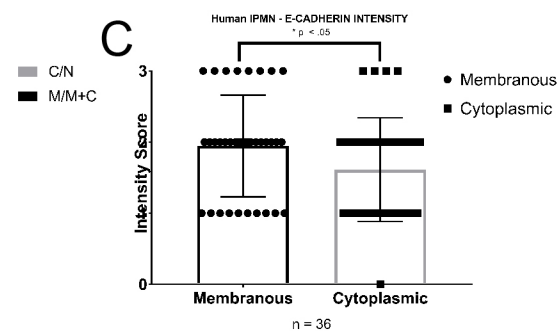
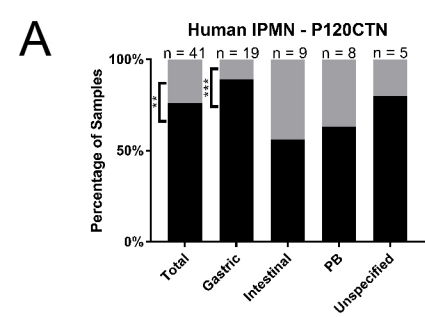
Kras^{G12D/wt}; Rosa26^{YFP}



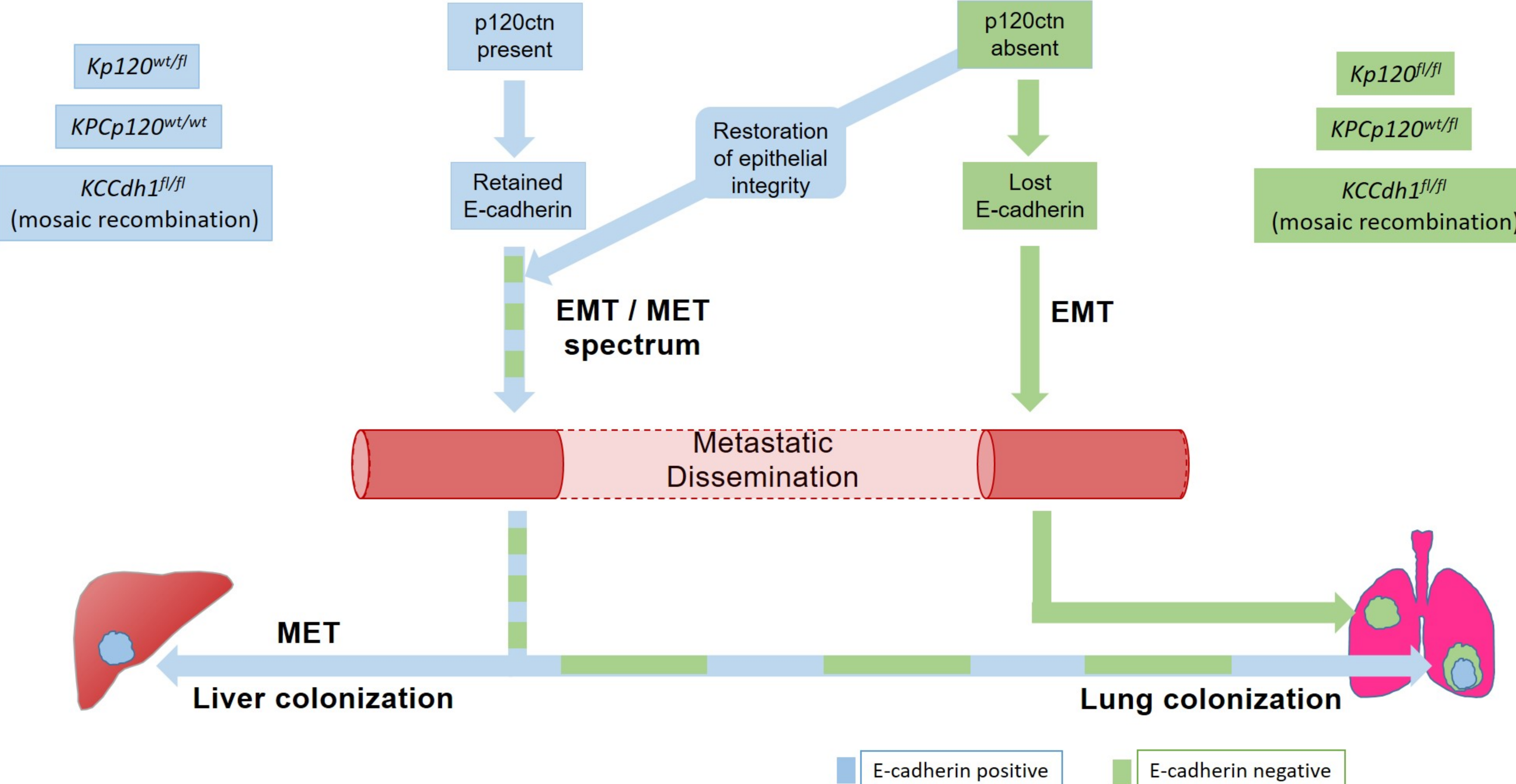
A**B**

Examples of Gross Pathology in Nude Mice 180 Days Post-Orthotopic Injection with *Kras*^{G12D/wt}; *p120ctn*^{w^t/fl}; *Rosa26*^{YFP} cells





The role of p120catenin in regulating the EMT-MET spectrum and metastatic organotropism in pancreatic cancer



<i>Pdx1-cre; KRAS^{G12D/+}</i>	Age (weeks)	Classification	Additional Notes
614	4.5	Normal	
616	4.5	Normal	
1328	6	Acinar Atrophy	Focal Necrosis
703	7	Normal	
799	8.2	Normal	
540	8.3	Normal	
1349	9.4	PanIN1A	
1346	9.4	Normal	
658	10	Normal	
981	11	Normal	
1099	11	PanIN1A	
702	13.2	Normal	
313	15	PanIN1A/IPMN-like dilation	IPMN-like dilatation of pancreatic duct
414	16	Normal	
1304	16.6	Normal	
390	18	Normal	
633	19.1	Ductalization	
1274	20	PanIN1A	
335	22.9	ADM	
1258	23.7	PanIN1B	
1257	23.7	Focal Duct Dilation	
1252	23.7	ADM	
316	23.9	PanIN1A	
1210	32.8	PanIn1A	
1179	35.7	Normal	
1178	35.7	PanIN1A	
1177	35.7	PanIN1A	
1176	35.7	PanIN1A/1B	
1175	35.7	PanIN1A/1B	
1103	40-50	PanIN1A	
1101	40-50	PanIN1A/1B	
7548	58	PanIN1A/1B	

Table S1: Detailed Breakdown of Classification of 32 *Pdx1-cre; KRAS^{G12D/+}* Mice

<i>Pdx1-cre; KRAS^{G12D/+}; p120ctn^{+/-fl}</i>	Age (weeks)	Classification	Additional Note
238	3	Ductalization	
607	5	Ductalization	
696	5	Normal	
243	6	PanIN3 associated with cystic changes	
1125	7.9	Normal	
648	8	Normal	
995	8	PanIN1A	
869	9.4	PanIN1B	
520	9.5	PanIN1B/IPMN-like change	Branch duct IPMN-like multilocular cystic lesion with low grade mucinous lining.
1023	10	Normal	
516	10.7	Ductalization	
515	11	Normal	
334	14	PanIN1B/IPMN-like change	Branch duct IPMN-like multilocular cystic lesion with low grade mucinous lining.
1040	14	PanIN1A/IPMN-like change	
597	17	Normal	
346	20	PanIN1A	
248	20	PDAC	Liver metastasis present.
354	20	PDAC	
685	21.1	PanIN1B	
680	21.1	PanIN1B	
686	21.1	PanIN1B/MCN	
369	21.6	PanIN1B	
366	22	Normal	
340	23.9	PanIN1B	
322	25.4	Normal	
327	25.7	PanIN1B	
557	30	Normal	
244	33.5	MCN	

1074	34.1	MCN	possible MCN? Periepithelial stroma + and epithelium mostly nonmucinous
1063	34.6	PanIN1A & 1B/MCN	possible MCN, focal sarcomatoid tumour
753	35	IPMN-like change	
1187	35.4	PanIN1B	Pseudoneoplastic islet cell hyperplasia
1183	35.4	PanIN1B	Pseudoneoplastic islet cell hyperplasia
1035	39.1	PanIN1B	
1104	42.3	PanIN1B	
1067	44.1	PanIN1B	possible sarcoma, small focus; Pseudoneoplastic islet cell hyperplasia
1038	40-50	PanIN1B	
990	55.7	PanIN1B/IPMN-like change	marked dilatation of main duct the head (ipmn like changes?); Pseudoneoplastic islet cell hyperplasia

Table S2: Detailed Breakdown of Classification of 38 *Pdx1-cre; KRAS^{G12D/+}; p120ctn^{+/-fl}* Mice

<i>Pdx1-cre; KRAS^{G12D/+}; p53^{+/-fl}</i>	Age (weeks)	Lung	Liver
1087	16	0	7
1096	13.3	2	14
1353	9.7	0	0
1344	0-10	0	19
1276	13.1	Infarcted	Infarcted
1236	17.7	Infarcted	Infarcted
1303	16.9	0	0
2032	25	0	0
2061	23	1	1
2041	38.7	2	0
PD 437	Unknown	0	1
PD 9238	15.8	0	18
PD 8078	27.1	564	1
PD 8963	Unknown	3	72
PD 9402	13.8	0	1
PD 422	34.2	0	7
PD 431	31.1	0	6
PD 635	23	1	8

Table S3: Quantification of Metastatic Burden in 18 *Pdx1-cre; KRAS^{G12D/+}; p53^{+/-fl}* Mice Used for Determination of Liver or Lung Dominance

<i>Pdx1-cre; KRAS^{G12D/+}; p53^{+/-}; p120ctn^{+/-}</i>	Age (weeks)	Lung	Liver
958	6	0	0
1037	17	3	0
1072	17	Saturated - Unquantifiable	0
1355	9.7	0	0
2113	11.5	0	0
2126	23.9	2 (including one large macroscopic metastasis)	0
2143	22.7	0	3
2173	11.3	0	0
2187	14.9	1	1
2278	19	1 (including one large macroscopic metastasis)	0

Table S4: Quantification of Metastatic Burden in 10 Pdx1-cre; KRAS^{G12D/+}; p53^{+/-}; p120ctn^{+/-} Mice Used for Determination of Liver or Lung Dominance

Cell Line	Transplantation Set	Mouse ID	Days post-injection	Tumor Penetrance	Liver Metastasis	Lung Metastasis
791Y	B	20	70	Yes	No	No
791Y	B	23	70	Yes	No	Yes
791Y	B	26	57	No	N/A	N/A
791Y	L	14	95	Yes	No	Yes
791Y	L	16	76	Yes	No	Yes
288Y	C	1	84	Yes	No	Yes
288Y	C	2	75	Yes	No	Yes
288Y	C	4	102	No	N/A	N/A
288Y	C	5	102	Yes	No	No
288Y	C	6	99	Yes	No	No
288Y	C	7	99	Yes	No	No
288Y	C	44	98	Yes	No	Yes

Table S5: Detailed Classification of all Long-Term Orthotopic Transplantation with *KRAS*^{G12D/+}; *p120ctn*^{fl/fl}; *Rosa26*^{YFP} Cells

Cell Line	Transplantation Set	Mouse ID	Days post-injection	Tumor Penetrance	Liver Metastasis	Lung Metastasis
791Y	A	8	84	Yes	No fluorescence available, but no	No fluorescence, excluded
791Y	A	10	62	Yes	No fluorescence available, but no	No fluorescence, excluded
791Y	A	11	79	Yes	Yes	No fluorescence, excluded
791Y	B	24	70	Yes	Yes	Yes
791Y	B	24	70	Yes	Yes	Yes
791Y	B	27	67	Yes	Yes	Yes
791Y	G	30	93	Yes	Yes	Yes
791Y	G	31	52	Yes	Yes	Yes
791Y	G	33	49	Yes	Yes	Yes
791Y	G	34	46	Yes	Yes	Yes
288Y	C	8	88	Yes	No	No
288Y	C	9	88	Yes	No	No
288Y	C	10	88	Yes	No	Yes
288Y	C	11	80	Yes	No	No
288Y	C	13	70	Yes	No	Yes
288Y	C	45	82	Yes	No	No
288Y	C	46	82	Yes	No	No

Table S6: Detailed Classification of all Long-Term Orthotopic Transplantation with *KRAS*^{G12D/+}; *p120ctn*^{fl/fl}; *Rosa26*^{YFP} Cells Rescued with p120ctn1A

ID Metastasis	ID Primary tumor	Date of birth	age	Gender (0=female, 1= male)	CTX (0=no, 1=yes)
E/2014/10393	E/2014/10393	2/22/1971	46	0	0
E/2014/794	E/2014/794	9/1/1968	49	1	1
E/2014/13508	E/2014/13508	11/17/1957	60	1	0
E/2013/34659	E/2013/34659	4/25/1939	78	0	0
E/2013/33897	E/2013/33897	1/4/1948	69	1	0
E/2013/31750	E/2013/31750	11/26/1941	75	1	0
E/2013/31749	E/2013/31749	12/28/1965	51	1	1
E/2013/31457	E/2012/016585	4/20/1963	54	0	0
E/2013/28594	E/2013/28594	11/12/1934	83	0	0
E/2013/18357	E/2013/035750	2/4/1951	66	0	1
E/2013/028825	E/2008/007691	12/1/1938	78	0	0
E/2013/002879	E/2013/002879	6/8/1956	61	0	0
E/2012/37959	E/2011/46424	2/1/1941	76	1	0
E/2012/13235	E/2011/28673	10/2/1949	68	1	0
E/2012/6665	E/2012/6665	12/14/1957	59	0	1
E/2012/002947	E/2012/3115	3/24/1961	56	0	0
E/2011/046143	E/2011/008097	10/14/1950	67	1	0

Table S7: Characteristics of Human Tumor Microarray